Centrifuge modeling of structure-soil-structure interaction: Seismic performance of inelastic building models

N.W. Trombetta & T.C. Hutchinson
University of California, San Diego, USA

H.B. Mason
Oregon State University, USA

J.D. Zupan & J.D. Bray
University of California, Berkeley, USA

C. Bolisetti & A.S. Whittaker
University at Buffalo, State University of New York, USA

Z. Chen
University of Missouri, Kansas City, USA

B.L. Kutter
University of California, Davis, USA

SUMMARY:
During an earthquake, adjacent buildings interact with each other through the surrounding soil. This phenomenon is referred to as structure-soil-structure interaction (SSSI). SSSI effects can be both beneficial and detrimental with respect to the seismic response of soil-foundation-superstructure (SFS) systems. Currently, SSSI effects are poorly understood by engineers because of a dearth of field data, experimental data, and analytical research. Consequently, SSSI effects are usually not considered during the seismic design of most SFS systems. The authors have performed four experiments at the NEES@UC Davis centrifuge facility to investigate SSSI effects. This paper describes the two most recent centrifuge tests (Test-3 and Test-4) and their results.

Keywords: soil-foundation-structure interaction, structure-soil-structure interaction, inelastic frame response

1. INTRODUCTION

1.1. Motivation and Project Description

Traditional structural seismic design and analysis techniques have generally assumed that a soil-foundation-structure (SFS) system responds with a fixed-base (i.e., the foundations are perfectly bonded to the surrounding soil and soil compliance is ignored). In reality foundations are able to displace relative to the surrounding soil, resulting in a response that differs from the fixed-base condition. The various mechanisms that lead to the modified response are collectively referred to as soil-foundation-structure interaction (SFSI) effects, and modern design codes provide provisions for considering SFSI effects (e.g., FEMA-356, FEMA-440, ASCE 41). In urban environments SFS systems interact not only with the surrounding soil, but also with the adjacent SFS systems that are simultaneously interacting with the same soil. As a result, the realized response is further modified from the fixed-base assumption. These interactions between closely spaced structures are referred to as structure-soil-structure interaction (SSSI) or, sometimes in the literature, as dynamic cross-interaction. SSSI is not considered in any modern design code, a situation that arises directly from a knowledge limitation.

The *NEESR-SG: City Block* project is an on-going research study aimed at developing a large number of physical case histories from which the effects of SSSI on SFS system performance can be observed. To data, four large-scale geotechnical centrifuge tests have been performed. Test-1 and Test-2 were aimed at studying the baseline SFSI response and modified SSSI response, respectively, of two inelastic frame structures. The results of Test-1 are described in Mason et al. (2010) and Chen et al. (2010). Detailed comparison of both the geotechnical and structural aspects of Test-1 and Test-2 are presented in Mason et al. (2012) and Trombetta et al. (2012). Some key results from Test-3 and Test-4, which studied the interactions between an inelastic frame structure and an elastic rocking structure, are presented herein. During Test-3 and Test-4 four cases are considered, as detailed in Section 2: (Case I) the baseline response of each structure; (Case II) in-plane SSSI; (Case III) anti-plane SSSI; and (Case IV) combined in-plane SSSI and anti-plane SSSI.

1.2. Structure-Soil-Structure Interaction

Seismic SFSI has received much attention in the earthquake engineering literature, and interested readers can consult Kausel (2010) for a historical review. In contrast, there has historically been a paucity of SSSI research. Lou et al. (2011), in their review of available SSSI literature, broadly define SSSI as the dynamic interactions among a multi-structure system through the soil-ground. The mechanisms, as well as the severity, of these interactions are a function of many parameters, including: the types of structural systems and foundations; soil type and properties; spacing between structures; and the orientation of the set of structures relative to the direction of ground shaking. *Anti-plane SSSI* (*aSSSI*) arises when between an array of SFS systems is oriented perpendicular to the direction of ground shaking (Luco and Contesse 1973). *In-plane SSSI* (*iSSSI*) occurs when an array of SFS systems is oriented parallel to the direction of ground shaking. Structures constructed in urban areas will most likely be surrounded by many structures, and will experience a combination of both anti-plane and in-plane SSSI.

Analytical methods exist for considering the interactions between highly simplified SFS systems oriented in arrays perpendicular to ground particle motion (e.g., Luco and Contesse, 1973; Wong and Trifunac, 1975), in arrays parallel to ground particle motion (e.g., Lee and Wesley, 1973), and in multi-direction arrays (e.g., Lee and Wesley, 1973). To arrive at tractable solutions to these difficult problems, these analytical methods rely on a large number of simplifying assumptions. As a result, comparisons between analytical solutions and strong shaking data are less meaningful. This is primarily due to the contributions of inelastic SFS system response (e.g., structural yielding and nonlinear response of the soil) and nonlinear SFSI effects (e.g., foundation uplift) in recorded data. As a result, experimental research (e.g., Mizuno, 1980; Nakagawa et al., 1998; Kitada et al., 1999) and numerical studies (e.g., Mulliken and Karabilis, 1998; Padron et al., 2009; Ghergu and Ionescu, 2009; Bolisetti and Whittaker, 2011) are currently in the forefront of SSSI research. Unfortunately, prior experimental studies have relied on low-level excitation or substantial simplifications in order to achieve nearly linear-elastic results. In addition, the numerical studies listed suffer from a lack of case history data illustrating SSSI, which is needed to validate the results of their models. As of this writing only one such case history (Celebi, 1993a,b) is known by the authors to exist. A primary goal of the *City Block* project is to provide well-documented experimental data from which (1) major effects of SSSI on nonlinear soil and structural response during strong shaking may be elicited and (2) existing and future numerical models can be validated and developed.

2. EXPERIMENTAL OVERVIEW

2.1. Experimental Configurations and Goals

Seismic centrifuge modeling principles are well defined in the literature, and interested readers can refer to Kutter (1995) for a summary. Important scaling factors for the *City Block* project are further summarized in Mason et al. (2010). Both Test-3 and Test-4 were performed at a centrifuge scale of $N = 55$. For clarity, all results and dimensions presented herein are reported in *prototype scale* (as opposed to the recorded *model scale*). Both Test-3 and Test-4 were performed using sites consisting of uniformly dense ($D_r = 80\%$) and dry Nevada sand. One-dimensional ground shaking was applied to the site during each test (the direction parallel to ground particle shaking is denoted as the North-South direction herein). Two structural models, as shown in Figure 1x, were tested: MS2F_M and MS1F_SF80.

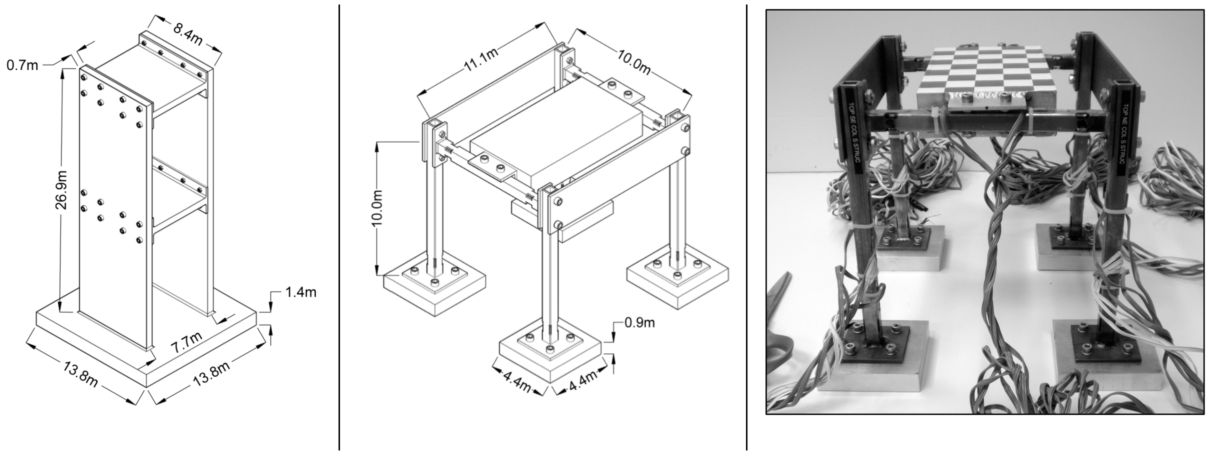

Figure 1. (a) Model MS2F_M and (b) Model MS1F_SF80 annotated with prototype scale dimensions. (c) Model MS1F_SF80 after strain gaging.

The design goals for MS1F_SF80 and MS2F_M were based on the objective of maximizing in-plane interaction between the structures during strong shaking events. Three main considerations influenced the structural designs: (1) the size of the two structures relative to each other, (2) the flexible-base periods (T^{SFSI}) of the structures relative to the site period, and (3) the susceptibility of the structures to inertial SFSI effects on their own. To this end, MS2F_M was designed to be much larger and heavier than MS1F_SF80. T^{SFSI} was chosen to be close to the estimated site period (0.6 sec) for both structures. Additionally, during the design of MS2F_M a number of parameters, such as effective height and total mass, were iterated upon until dimensionless parameters defined in the literature (e.g., Veletsos and Meek, 1974; Veletsos and Nair, 1975; and Stewart et al., 1999a,b) predicted that inertial interaction effects would be significant. MS1F_SF80 was designed such that the flexible-base strength properties of the frame, base shear-to-weight ratio (V_y/W) and roof drift (δ_y) at first structural yield, are within the bounds of realistic prototype structures. Detailed design procedures for both structures are presented in the Test-3 Data Report (Mason et al., 2011).

Parallel to ground shaking, MS2F_M responds as a two-degree-of-freedom elastic shear wall founded on a shallowly embedded mat. MS2F_M was designed such that during strong ground shaking it would respond primarily through foundation rocking (i.e., rigid superstructure response). In this configuration, the design fixed-base and SFSI modal parameters for MS2F_M are: $T_1^{FB} = 0.13\,sec$, $\beta_1^{FB} = 2.5\%$, $T_1^{SFSI} = 0.60\,sec$, and $\beta_1^{SFSI} = 36\%$. Perpendicular to ground shaking, MS2F_M responds as a two-degree-of-freedom elastic frame. Parallel to ground shaking, MS1F_SF80 responds as a single-degree-of-freedom inelastic frame founded on shallowly embedded individual spread footings. The cross-sectional area was reduced near the ends of the beams and at the base of each column to concentrate inelastic superstructure deformations at known locations. These locations are herein referred to as *fuses*. The design (i.e., undamaged) fixed base and SFSI modal parameters for MS1F_SF80 in this configuration are: $T_1^{FB} = 0.47\,sec$, $\beta_1^{FB} = 2.5\%$, $T_1^{SFSI} = 0.65\,sec$, and $\beta_1^{SFSI} = 5.1\%$. The design strength properties of MS1F_SF80 are: $V_y/W = 0.46$ and $\delta_y = 1.03\%$. Perpendicular to ground shaking, MS1F_SF80 responds as an elastic single-degree-of-freedom frame.

Within Test-3 and Test-4 four configurations were tested to observe the response of MS1F_SF80 with various boundary conditions. Case I is the baseline SFSI case, where MS1F_SF80 responds independently of the influence of another structure. Case II (Figure 2a) considers only in-plane SSSI, with MS1F_SF80 located directly south of MS2F_M. Case III (Figure 2b) considers only anti-plane SSSI, with MS1F_SF80 located directly west of MS2F_M. Case IV (Figure 2c) considers the combination of both in-plane and anti-plane SSSI, by placing MS1F_SF80 at the 'corner' of an L-shaped array. Cases I and II were tested concurrently (i.e., in the same centrifuge container, separated by a large distance) during Test-3. Cases III and IV were tested concurrently during Test-4. No baseline case for MS2F_M was recorded, as it was expected to be minimally influenced by the presence of MS1F_SF80 during either Case II or III.

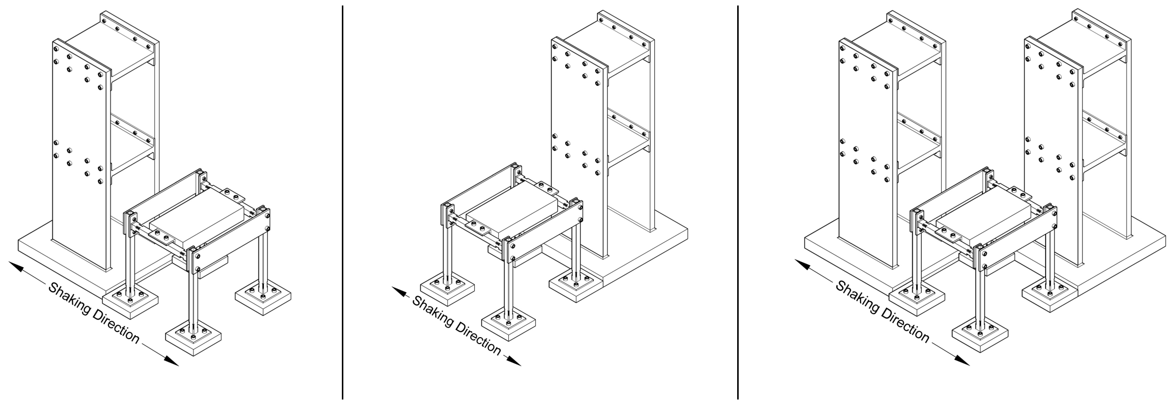

Figure 2. (a) Structural orientation during Case II: in-plane shaking. (b) Structural orientation during Case III: anti-plane shaking. (c) Structural orientation during Case IV.

2.2. Ground Motions

Mason et al. (2010, 2012) presents information regarding the motion selection and calibration processes for the *City Block* test series. During Test-3, 23 ground motions were applied to the Case I and II models. During Test-4, 18 ground motions were applied to the Case III and IV models. Table 1 presents a summary of the ground motion plans, as well as select intensity measures, for both tests. As demonstrated by the relative peak ground accelerations (*PGA*), peak ground velocities (*PGV*), and spectral acceleration ($S_{a,0.6}$) measurements from both tests; there was acceptable repeatability of each motion from test-to-test. Figure 3 displays representative spectral acceleration plots for the free-field ground motions measured at the surface of the model (Figure 3, top) at the base of the model (Figure 3, bottom). These plots demonstrate the wide variety of motions contained within the *City Block* ground motion database. Not demonstrated herein (but discussed in Mason et al. (2012)) is that the ground motion database also included a number of motions exhibiting near-fault characteristics, in addition to ordinary ground motions. It should be noted that Test-3 also includes a several applications of the JOS_L motion early in the test sequence. This was due to mechanical issues with the centrifuge and instrumentation performance during the initial checking stage of the test sequence.

3. ELICITATION OF SSSI EFFECTS: METHODOLOGY

3.1. Intensity Measure-Demand Parameter Relationships

Earthquake motion intensity measures (IMs) are used to capture the salient features of an earthquake motion time series (i.e., acceleration, velocity, and displacement). Intensity measures usually capture the amplitude, frequency content, or duration of an earthquake motion, though some intensity measures capture two or all three of these important earthquake motion features. When using the Pacific Earthquake Engineering Research (PEER) Center's Performance Based Earthquake Engineering (PBEE) framework, earthquake motion intensity measures are correlated to structural demand parameters (DPs), and the DPs are connected to loss (via damage states and consequence functions (ATC, 2012). DPs are chosen so that they can generally be correlated to a level of damage within the structure, such as component yielding, non-structural component damage, or even collapse. The relationship between a specific IM and DP can vary for the same superstructure, depending on soil and foundation conditions, as discussed by Kramer (2011). So it follows that the IM-DP relationship for a specific structure should be modified by the presence of SSSI effects. Herein, we compare the MS1F_SF80 IM-DP relationship for each of the four tested cases, for a variety of IMs and DPs. The resulting deviations from the baseline relationship can be attributed to SSSI.

3.2. Selected Intensity Measures

Four simple measures of ground motion intensity were chosen for this study: peak ground acceleration (*PGA)*, peak ground velocity (*PGV)*, spectral acceleration at the design (i.e., undamaged) period and damping ratio for each structure (S_a), and spectral acceleration at the identified first mode period and damping ratio for each structure (S_a^{ID}). The mathematical definitions of the chosen intensity measures are given in Equations 3.1 through 3.4:

$$PGA = max(|\ddot{\Delta}_g^x|) \tag{3.1}$$
$$PGV = max(|\dot{\Delta}_g^x|) \tag{3.2}$$
$$S_a = S_a(T_1^{SSI}, \beta_1^{SSI}) \tag{3.3}$$
$$S_a^{ID} = S_a(T_1^{ID}, \beta_1^{ID}) \tag{3.4}$$

Where Δ_g^x is the horizontal displacement of the free-field soil surface (with $\ddot{\Delta}_g^x$ and $\dot{\Delta}_g^x$ respectively representing the free-field surface acceleration and velocity), T_1^{SFSI} is the design first mode period, β_1^{SFSI} is the design first mode damping ratio, T_1^{ID} is the experimentally identified motion specific first mode period, and β_1^{ID} is the experimentally identified motion specific first mode damping ratio. T_1^{ID} and β_1^{ID} are referred to herein as the *motion specific modal parameters*, and are identified for each structure on a motion-by-motion basis using the methodologies described by Chen et al. (2012).

The four chosen intensity measures are broken down into two categories. The IMs *PGA* and *PGV* do not take into account the properties of MS1F_SF80, but only consider the properties of the ground motion itself. S_a and S_a^{ID} account for the expected and realized modal parameters respectively of the SFS system, in addition to the frequency content and amplitude of the ground motion. Although many other measures of ground motion intensity exist in the literature, these four intensity measures were chosen to demonstrate how SSSI can modify the IM-DP relationship of a specific structure due to both their simplicity and predictive power.

Table 1. Test-3 and Test-4 Ground Motions

Test-3 ID	Test-4 ID	Motion Name	Test-3 Surface / Test-4 Surface		
			PGA (g)	PGV (cm/sec)	$S_{a,0.6}$ (g)†
1	1	JOS_L	0.13 / 0.12	17 / 16	0.55 / 0.51
2	-	JOS_L	0.14 / -	17 / -	0.55 / -
3	2	TCU_L	0.21 / 0.23	21 / 20	0.48 / 0.48
4	-	JOS_L	0.15 / -	17 / -	0.61 / -
5	-	JOS_L	0.14 / -	16 / -	0.54 / -
6	-	TCU_L	0.22 / -	21 / -	0.50 / -
7	3	RRS	0.34 / 0.32	54 / 52	0.68 / 0.65
-	4	JOS_L	- / 0.13	- / 16	- / 0.53
8	5	PTS	0.21 / 0.20	27 / 28	0.78 / 0.81
9	6	SCS_L	0.26 / 0.28	31 / 33	0.91 / 0.89
10	7	LCN	0.31 / 0.32	50 / 49	0.69 / 0.71
11	8	WVC_L	0.38 / 0.34	48 / 47	1.00 / 1.07
12	9	SCS_H	0.61 / 0.50	71 / 68	2.46 / 2.40
13	10	PRI*	0.83 / 0.81	68 / 65	1.70 / 1.82
-	11	PRI_55**	- / 0.55	- / 79	- / 1.31
14	12	JOS_L	0.16 / 0.16	16 / 17	0.55 / 0.60
15	13	JOS_L	0.15 / 0.15	16 / 17	0.56 / 0.58
16	14	JOS_H	0.46 / 0.53	52 / 52	2.24 / 2.21
17	15	WPI	0.40 / 0.38	59 / 57	0.68 / 0.69
18	16	TCU_H	0.47 / 0.54	39 / 34	0.91 / 0.94
19	17	WVC_H	0.47 / 0.40	67 / 68	1.32 / 1.35
20	-	SCS_H	0.79 / -	80 / -	2.65 / -
21	-	PRI*	0.70/-	73 / -	1.82 / -
22	-	SCS_H	0.79/-	80 / -	2.86 / -
23	18	JOS_L	0.18 / 0.17	17 / 17	0.61 / 0.64

*Includes only half the desired frequency content
**Correctly scaled to include all of the desired frequencies
† $S_{a,0.6} = S_a(T = 0.6 \text{ sec}, \beta = 5\%)$

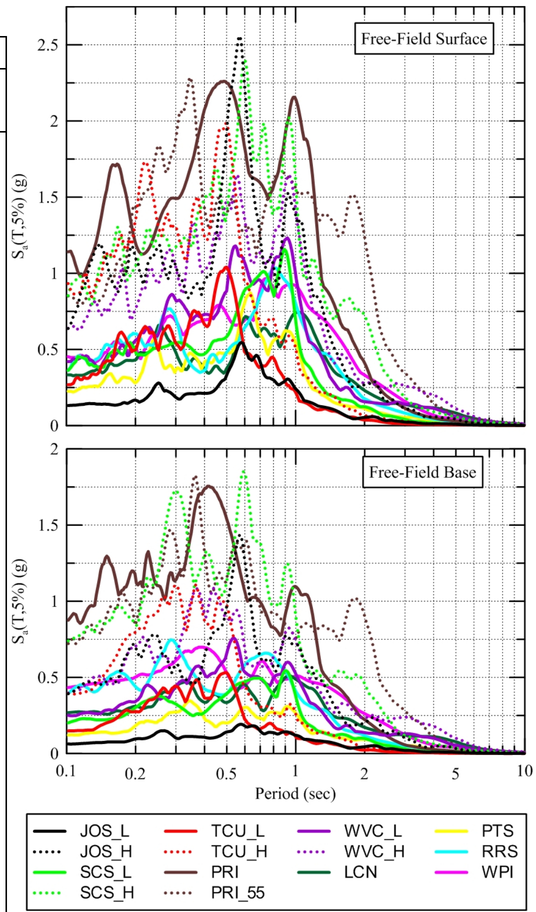

Figure 3. 5% damping acceleration response spectra for (top) the free-field surface and (bottom) free-field input motions

3.3. Selected Demand Parameters

The total horizontal roof displacement of a single story two-dimensional single-bay frame founded on shallow spread footings is defined by the following equation:

$$\Delta_T^x = \Delta_g^x + \Delta_s^x + avg\left(\delta_{F_n}^x, \delta_{F_{n+1}}^x\right) + \alpha_{n,n+1}h_s + avg\left(\theta_{F_n}, \theta_{F_{n+1}}\right)h_s \tag{3.5}$$

Where Δ_T^x is the total horizontal roof displacement; Δ_g^x is the horizontal ground surface displacement; Δ_s^x is the horizontal roof displacement due to structural deformation; $\delta_{F_n}^x$ is the sliding of Footing 'n' (above the ground surface displacement); $\alpha_{n,n+1}$ is the angle of differential settlement between Footings 'n' and 'n+1'; θ_{F_n} is the angle of rotation of Footing 'n' (less the contribution of differential settlement); and h_s is the height of the structure. It is expected that the contributions of sliding and differential settlement to the total roof displacement will be minimal compared to individual foundation rocking and structural deformation, but these terms are included here for completeness. By twice differentiating Equation 3.5 a similar expression is obtained for the total roof acceleration:

$$\ddot{\Delta}_T^x = \ddot{\Delta}_g^x + \ddot{\Delta}_s^x + avg\left(\ddot{\delta}_{F_n}^x, \ddot{\delta}_{F_{n+1}}^x\right) + \ddot{\alpha}_{n,n+1}h_s + avg\left(\ddot{\theta}_{F_n}, \ddot{\theta}_{F_{n+1}}\right)h_s \tag{3.6}$$

Where the double-dot superscripts (i.e., $\ddot{\Delta}$) indicate a displacement or rotation time series that has been twice differentiated to obtain an acceleration or rotational acceleration measurement. The contributions of individual rocking, ground acceleration, and structural deformation are again expected to be the largest contributors to total roof acceleration.

Five seismic demand parameters were chosen for this study: peak roof acceleration (*DP1*), peak roof drift (*DP2*), roof drift due to peak footing sliding (*DP3*), roof drift due to peak footing rotation (*DP4)*, and peak beam fuse ductility (*DP5*). These five parameters are defined numerically in Equations 3.7 through 3.11:

$$DP1 = max\left(\left|\ddot{\Delta}_T^x\right|\right) \tag{3.7}$$

$$DP2 = max(|\Delta_T^x\ |)/h_s * 100\% \tag{3.8}$$

$$DP3 = max\left(max\left(\left|\delta_{F_1}^x\right|\right), max\left(\left|\delta_{F_2}^x\right|\right), max\left(\left|\delta_{F_3}^x\right|\right), max\left(\left|\delta_{F_4}^x\right|\right)\right)/h_s\ * 100\% \tag{3.9}$$

$$DP4 = max\left(max\left(\left|\theta_{F_1}^x\right|\right), max\left(\left|\theta_{F_2}^x\right|\right), max\left(\left|\theta_{F_3}^x\right|\right), max\left(\left|\theta_{F_4}^x\right|\right)\right) * 100\% \tag{3.10}$$

$$DP5 = max\left(max(|\phi_1|), max(|\phi_2|), max(|\phi_3|), max(|\phi_4|)\right)/\phi_y \tag{3.11}$$

Where the displacement and acceleration measurements have been defined previously, ϕ_n is the curvature of beam fuse 'n', and ϕ_y is the yield curvature of the beam fuse cross-section.

4. ELICITATION OF SSSI EFFECTS: RESULTS

4.1. Instrumentation and Data Processing

Each MS1F_SF80 model was densely instrumented with accelerometers, linear potentiometers, and strain gages during each test. In general, each MS1F_SF80 model was instrumented with three accelerometers on each footing (i.e., one horizontal to capture sliding and two vertical to capture settlement and rotation) and at least one horizontal accelerometer at the roof (i.e., to capture total roof motion). Linear potentiometers were placed in similar locations to the accelerometers to capture displacement. However, due to DAQ channel constraints, each acceleration measurement could not be complemented with a corresponding linear potentiometer. Strain gages were placed in pairs at each fuse location and near the top of each column, with one gage on each opposing bending face of the structural component. This strategy allowed for the average curvature of the instrumented cross-section, and therefore the localized inelastic response at each fuse, to be captured. Full instrumentation plans for both Test-3 and Test-4 can be found in their respective centrifuge data reports (Mason et al., 2011; Trombetta et al., 2011)

Data was collected at a model scale rate of 4096 Hz, which corresponds to approximately 75 Hz at prototype scale. Prior to extracting demand parameters or calculating intensity measures each record was filtered and, if necessary, treated with baseline correction in accordance with the strategies outlined in Trombetta et al. (2012). In addition to the DAQ channel constraints mentioned above, the acceleration measurements generally proved to be more reliable than their corresponding displacement measurements. As a result, the displacement results presented herein are computed from double integrated accelerometer measurements. These measurements are therefore representative of the *transient* displacement of each location (i.e., they do not contain information about the residual displacements), and are expected to be approximately representative of, but not identical to, the achieved inelastic displacements of the SFS systems.

4.2. Observed IM-DP Relationships

Each of the four selected intensity measures was compared against each of the five selected demand parameters for each of the four cases: (I) the baseline MS1F_SF80 response; (II) the iSSSI-influenced MS1F_SF80 response; (III) the aSSSI-influenced response; and (IV) the response of MS1F_SF80 under the combined influence of iSSSI and aSSSI. These results are aggregated in Figure 4. During disassembly of the Test-4 model, it was observed that the Case III MS1F_SF80 floor mass has shaken itself slightly loose from its connections to the beams. Large spikes in the recorded roof acceleration measurements were observed during data post-processing, and are attributed to the small amount of sliding that may have occurred between the floor mass and the beams. As a result, IMs and DPs that rely directly on roof acceleration (DP1, DP2, and S_a^{ID}) are omitted for Case III.

The data points in Figure 4 are presented alongside either a simple linear (i.e., $DP = a * IM + b$) or exponential (i.e., $ln(DP) = d * IM + c$) fit. A linear fit was utilized for each comparison except for those involving the peak curvature ductility (Figures 4q-4t). An exponential fit was used for these comparisons due to the observed shape of the data. For many of the other correlations a nonlinear fit may be more appropriate than the displayed linear fits, but only linear fits are presented in Figure 4a through Figure 4p for simplicity. Additionally, the calculated coefficients have not been reported herein, as the fits provided are not meant to hold predictive power, but only illustrate trends in the data.

Figures 4a through 4d present the correlations between the recorded peak roof accelerations (DP1) and each of the four IMs. It is observed from these plots that Case II results in larger roof accelerations than the baseline case, while the effects of combined iSSSI and aSSSI (Case IV) result in decreased peak roof accelerations. Similarly, peak roof displacements (Figures 4e through 4h) are increased for Case II compared to the baseline case. Case IV results in increased peak roof displacements as well, in contrast to the peak roof acceleration trends. These results indicate that SSSI can affect two DPs that are closely associated with structural (DP2) and non-structural damage (DP1).

The results for the peak roof drift due to the contribution of footing sliding (DP3) are more complicated. The linear fits in Figures 4i and 4k suggest that each Case II, Case III, and Case IV result in increased, compared to the baseline case, sliding demands during strong shaking. In contrast, the fits in Figure 4j and 4l suggest that Case III and Case IV deamplify the sliding contribution during large motions. Mixed results are also observed for the peak roof drift due to the contribution of footing rotation (DP4), although the trends illustrated in Figures 4m, 4n and 4o suggest that each Case II, Case III and Case IV result in larger footing rotations than the baseline case during strong motions.

The results for the peak beam curvature ductility (DP5) suggest that the SSSI effects arising in Case II may slightly increase the observed damage, while Case III may result in slightly reduced structural damage. Most notably, the results from Case IV suggest that combined aSSSI and iSSSI effects result in significantly reduced structural damage over the baseline case. These results are consistent across all four selected intensity measures for the model structures and soil conditions described herein.

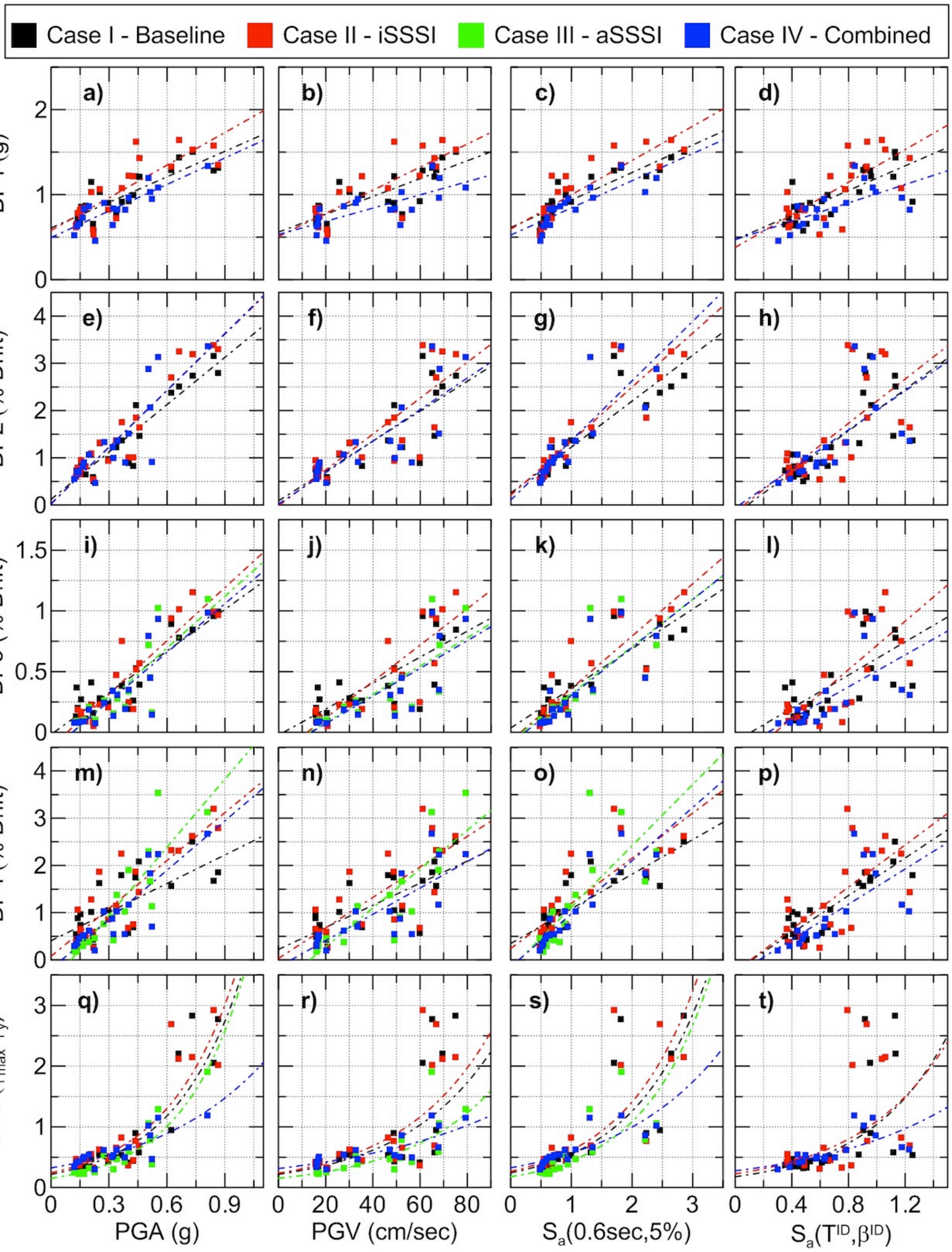

Figure 4. Intensity measure vs. demand parameter correlations for MS1F_SF80 for Case I (black markers), Case II (red markers), Case III (green markers), and Case IV (blue markers). Each data set is accompanied by either a linear ($\boldsymbol{DP = a * IM + b}$) or exponential ($\boldsymbol{ln(DP) = d * IM + c}$) fit.

5. CONCLUSIONS

During two geotechnical centrifuge experiments (Test-3 and Test-4) four identical inelastic model structures (MS1F_SF80) was exposed to strong ground shaking under a variety of boundary conditions. During Test-3, the baseline response of MS1F_SF80 was recorded (Case I). Simultaneously, the response of MS1F_SF80 was recorded while subjected to the effects of in-plane SSSI (Case II). During Test-4, two additional cases were studied. First, the response of MS1F_SF80 was recorded while subjected to the effects of anti-plane SSSI (Case III). Second, the response of MS1F_SF80 was recorded while subject to simultaneous iSSSI and aSSSI effects (Case IV). The results of these two tests are presented herein in the form of IM-DP correlations. The observed results are mixed (i.e., the effects of iSSSI do not unilaterally increase the peak demand parameters, aSSSI does not unilaterally result in decreased demand parameters, etc.), and the observed trends are necessarily dependent on the chosen ground motion database and local soil conditions.

The results do illustrate that SSSI effects, arising from either an in-plane or anti-plane orientation of a structural array, can significantly alter the response of an urban structure. The data indicates that SSSI effects can modify the baseline IM-DP correlations for an inelastic structure, given the selected ground motion database, soil conditions, and relative structural locations. Ultimately, these modified relationships between ground motion intensity and structure-foundation demands will result in modified relationships between ground motion intensity measures and structural damage levels as well. Further experimental work, both physical and numerical, is currently being pursued by the *City Block* team in an attempt to generalize the observed trends beyond the four cases presented to account for a larger ground motion database, a variety of soil conditions, and additional structural array configurations.

ACKNOWLEDGEMENT

This material is based upon work supported by the National Science Foundation under Grant No. CMMI-0830331. Any opinions, findings, and conclusions or recommendations expressed in this material are those of the authors and do not necessarily reflect the views of the National Science Foundation. Experiments were conducted at the Center for Geotechnical Modeling at the University of California at Davis, which is supported by the NSF George E. Brown, Jr. Network for Earthquake Engineering Simulation (NEES) program under Award No. CMMI-0402490. The authors gratefully acknowledge the assistance of the UCD staff and in particular Dan Wilson, Ray Gerhard, and Anatoliy Ganchenko. We would also like to give credit for the substantial assistance of the principal investigators and other researchers involved with this research grant, but not listed in the authorship: Gregg Fiegel, Katherine Jones, Hamilton Puangnak, Patrick Bassal, Jeannie Tran, Johnny Lund, Stefanie Gille and Robert Reitherman. Finally, we would like to acknowledge the contributions of our professional practice committee: Marshall Lew, Mark Moore, Farzad Naeim, Farhang Ostadan, Paul Somerville, and Michael Willford.

REFERENCES

Applied Technology Council (ATC). (2012). Guidelines for the seismic rehabilitation of buildings, Report No. ATC-58-1, Redwood City, CA.

Bolisetti, C. and Whittaker, A. S. (2011). Seismic structure-soil-structure interaction in nuclear power plant structures. *Transactions*, 21st International Conference on Structural Mechanics in Reactor Technology (SMiRT 21), Paper 228, New Delhi, India.

Celebi, M. (1993). Seismic responses of two adjacent buildings: Data and analyses. *ASCE Journal of Structural Engineering*. **119**, 2461-2476.

Celebi, M. (1993). Seismic response of two adjacent buildings: Interaction. *ASCE Journal of Structural Engineering*. **119**, 2477-2492.

Chen, Z., Hutchinson, T.C., Trombetta, N.W., Mason, H.B., Bray, J.D., Jones, K.C., Bolisetti, C., Whittaker, A.S., Choy, B.Y., Kutter, B.L., Fiegel, G.L., Montgomery, J., Patel, R.J., and Reitherman, R. (2010). Seismic Performance Assessment in Dense Urban Environments: Evaluation of Nonlinear Building-Foundation Systems using Centrifuge Tests. *Fifth International Conference on Recent Advances in Geotechnical Earthquake Engineering and Soil Dynamics*.

Chen, Z., Trombetta, N.W., Hutchinson, T.C., Mason, H.B., Bray, J.D., Kutter, B.L., and Whittaker, A.S. (2012, in review). Seismic soil-structure system identification for a centrifuge-based nonlinear building model - Part a: Framework and verification. *Soil Dynamics and Earthquake Engineering.* **In review**.

Ghergu, M. and Ionescu, I.R. (2009). Structure-soil-structure Coupling in Seismic Excitation and `City Effect'. *International Journal of Engineering Science*. **47**, 342-354.

Kausel, E. (2010). Early history of soil-structure interaction. *Soil Dynamics and Earthquake Engineering*. **30**, 822-832.

Kitada, Y., Hirotani, T., and Iguchi, M. (1999). Models test on dynamic structure-structure interaction of nuclear power plant buildings. *Nuclear Engineering and Design*. **192**, 205-216.

Kramer, S. L. (2011). Performance-based design in geotechnical earthquake engineering practice. *5th International Conference on Earthquake Geotechnical Engineering.*

Kutter, B.L. (1995). Recent Advances in Centrifuge Modeling of Seismic Shaking. *Third International Conference on Recent Advances in Geotechnical Earthquake Engineering and Soil Dynamics*.

Lee, T.H. and Wesley, D.A. (1973). Soil-structure interaction of nuclear reactor structures considering through-soil coupling between adjacent structures. *Nuclear Engineering and Design*. **24**, 374 - 387.

Lou, M., Wang, H., Chen, X., and Zhai, Y. (2011). Structure-soil-structure interaction: Literature review. *Soil Dynamics and Earthquake Engineering.* **31**, 1724-1731.

Luco, J.E. and Contesse, L. (1973). Dynamic structure-soil-structure interaction. *Bulletin of the Seismological Society of America*. **63**, 1289-1303.

Mason, H.B., Bray, J.D., Jones, K.C., Chen, Z., Hutchinson, T.C., Trombetta, N.W., Choy, B.Y., Kutter, B.L., Fiegel, G.L., Montgomery, J., Patel, R.J., Reitherman, R., Bolisetti, C., and Whittaker, A.S. (2010). Earthquake Input Motions and Seismic Site Response in a Centrifuge Test Examining SFSI Effects. *Fifth Inter. Conf. on Recent Adv. in Geotechnical EQ Engineering & Soil Dynamics*.

Mason, H.B., Trombetta, N.W., Gille, S.M., Lund, J.N, Zupan, J.D., et al. (2011). Seismic performance assessment in dense urban environments: centrifuge data report for HBM04. Technical report, Center for Geotechnical Modeling, University of California, Davis.

Mason, H.B., Trombetta, N.W., Chen, Z., Bray, J.D., Hutchinson, T.C., and Kutter, B.L. (2012, in review). Seismic soil-foundation-structure interaction observed in geotechnical centrifuge experiments. *Soil Dynamics and Earthquake Engineering*. **In review.**

Mizuno, H. (1980). Effects of structure-soil-structure interaction during various excitations. *7th World Conference on Earthquake Engineering*. 149-156.

Mulliken, J.S. and Karabalis, D.L. (1998). Discrete model for dynamic through-the-soil coupling of 3-D foundations and structures. *Earthquake Engineering & Structural Dynamics*. **27**, 687-710.

Nakagawa, S., Kuno, M., Naito, Y., Nozawa, T., Momma, T., Mizuno, J., Tsukamoto, T., Motohashi, S., and Niwa, M. (1998). Forced vibration tests and simulation analyses of a nuclear reactor building. *Nuclear Engineering and Design*. **179,** 145-156.

Padron, L.A., Aznarez, J.J. and Maeso, O. (2009). Dynamic structure-soil-structure interaction between nearby piled buildings under seismic excitation by BEM-FEM model. *Soil Dynamics and Earthquake Engineering*, **29**, 1084 - 1096.

Stewart, J. P, Fenves, G. L., and Seed. R. B. (1999a). Seismic soil-structure interaction in buildings. I: analytical methods, *Journal of Geotechnical and Geoenvironmental Engineering,* **125**, 26-37.

Stewart, J. P., Seed, R. B., and Fenves, G. L. (1999b). Seismic soil-structure interaction in buildings. II: empirical findings, *Journal of Geotechnical and Geoenvironmental Engineering,* **125**, 38-48.

Trombetta, N.W., Zupan, J.D., Bolisetti, C., Puangnak, H., Jones, K.C., et al. (2011). Seismic performance assessment in dense urban environments: centrifuge data report for NWT01. Technical report, Center for Geotechnical Modeling, University of California, Davis.

Trombetta, N.W., Mason, H.B., Chen, Z., Hutchinson, T.C., Bray, J.D., and Kutter, B.L. (2012, in review). Nonlinear dynamic foundation and frame structure response observed in geotechnical centrifuge experiments. *Soil Dynamics and Earthquake Engineering.* **In review.**

Veletsos, A. S. and Meek, J. W. (1974). Dynamic behaviour of building-foundation systems, *Earthquake Engineering and Soil Dynamics,* **3**, 121-138.

Veletsos, A. S. and Nair, V. D. (1975). Seismic interaction of structures on hysteretic foundations, *Journal of the Structural Division,* **101(ST1)**, 109-129.

Wong, H.L and Trifunac, M.D. (1975). Two-dimensional, antiplane, building-soil-building interaction for two or more buildings and for incident planet SH waves, Bulletin of the Seismological Society of America. **65**, 1863-1885.